

# Domain nucleation in hard/soft ferromagnetic bilayers with exchange coupling through a pinhole

E. Saitoh, T. Nakamura, H. Matsumoto, and H. Miyajima

*Department of Physics, Keio University, Hiyoshi, Yokohama 223-8522, Japan*

(Received 5 February 2003; published 21 July 2003)

The magnetization process has been investigated for  $\text{SmCo}_5/\text{SiO}_2/\text{Fe}_{19}\text{Ni}_{81}$  trilayer films, in which the exchange coupling between the hard-ferromagnetic  $\text{SmCo}_5$  layer and the soft-ferromagnetic  $\text{Fe}_{19}\text{Ni}_{81}$  layer is controlled by the dimension of a small pinhole ( $10\text{--}100\ \mu\text{m}$  in diameter) penetrating the  $\text{SiO}_2$  layer. The magnetization curves and magnetic torque curves indicate that the magnetization reversal in the  $\text{SmCo}_5$  layer consists of a nucleation around the pinhole and the propagation of the domain wall. This is responsible for the suppression of the coercivity induced by the coupling through the pinhole.

DOI: 10.1103/PhysRevB.68.012409

PACS number(s): 75.70.Cn, 75.60.Jk

Exchange coupling arising from the interface between magnetic films has been of interest in the field of magnetism due to its underlying physics as well as its significance to application.<sup>1–5</sup> In the bilayer films composed of hard and soft ferromagnets, exchange coupling at the interface has been shown to produce versatile results including the enhancement of the energy product.<sup>6</sup> The exchange-coupling effect has phenomenologically been argued in terms of the competition between the width of the domain wall and the thickness of the layers.<sup>7</sup> In fact, the variation in the magnetization curve for hard/soft hybrid ferromagnetic bilayers with the film thickness is mostly enhanced when the thickness is close to the typical extension of the domain wall.<sup>7</sup> This implies that controlling the dimension of the interface to generate competition among the characteristic-length scales in the magnetic bilayers may also have further critical influence upon their magnetic properties. In this study, we investigated the magnetization process in hard/soft-ferromagnetic films by controlling the size of the interface. The results indicate that a micron-sized interface between hard-/soft-ferromagnetic films significantly increases the instabilities of the domain nucleation in the hard-ferromagnetic layer.

Figure 1(a) is a schematic illustration of the cross section and top views of the films adopted in the present study. The system consists of a hard-ferromagnetic  $\text{SmCo}_5$  layer, a non-magnetic  $\text{SiO}_2$  layer with a pinhole, and a soft-ferromagnetic  $\text{Fe}_{19}\text{Ni}_{81}$  layer. The size of the interface between the magnetic layers was controlled by changing the diameter of the pinhole ( $d=10\text{--}100\ \mu\text{m}$ ) penetrating the  $\text{SiO}_2$  layer. Hereafter the sample system  $\text{SmCo}_5/\text{SiO}_2/\text{Fe}_{19}\text{Ni}_{81}$  is designated in this paper as  $S_d$ , where the subscript  $d$  denotes the pinhole diameter in units of  $\mu\text{m}$ . The films were fabricated onto thermally oxidized Si substrates in four steps as follows. In the first step, a  $\text{SmCo}_5$  layer of 150-nm thickness and of 6.3-mm diameter was sputtered onto a substrate in an argon gas pressure of 5 mTorr. During the sputtering, the external magnetic field of 48 kA/m was applied to the film plane so as to induce a uniaxial magnetic anisotropy in the  $\text{SmCo}_5$  films. In the second step, a  $\text{SiO}_2$  layer of 50-nm thickness was deposited by electron-beam evaporation in an oxygen gas pressure of  $1\times 10^{-4}$  mTorr. In the third step, a resist (ZEP50) mask of  $0.1\text{-}\mu\text{m}$  thickness was dispersed onto the

$\text{SiO}_2$  layer by spin coating. After patterning a pinhole of 10- or  $100\text{-}\mu\text{m}$  diameter by using an electron-beam writer, the resist mask was developed. The  $\text{SiO}_2$  layer was etched through the pinhole using  $\text{CF}_4$  plasma. The shape of the pinhole penetrating the  $\text{SiO}_2$  layer was observed using a scanning electron microscope [see Figs. 1(b) and 1(c)]. Finally, after the resist mask was removed, the  $\text{Fe}_{19}\text{Ni}_{81}$  layer of 100-nm thickness was sputtered onto the  $\text{SiO}_2$  layer in an argon gas pressure of 5 mTorr. Before sputtering, to clean it, the surface was etched by an argon ion to 5 nm in depth. The chemical composition for each layer was analyzed by means of x-ray luminescence microscopy and showed an almost identical composition to the prescribed ratio. The magnetization curves and magnetic torque curves at 4.2 K were measured using a vibrating sample magnetometer and a magnetic torque magnetometer with a torque sensitivity up to  $5\times 10^{-8}$  N·cm.

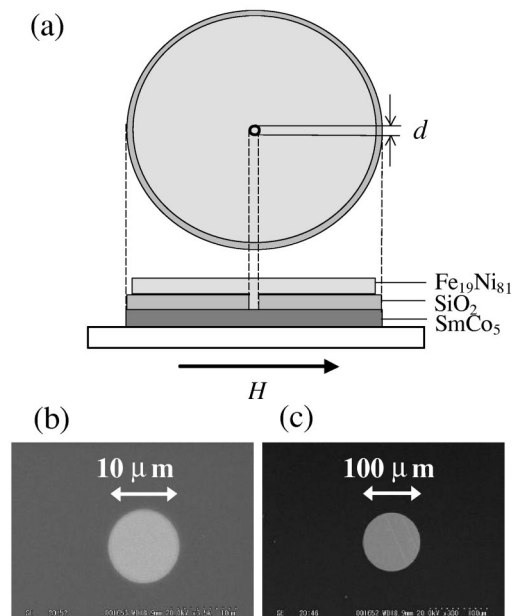


FIG. 1. (a) Schematic illustration of the cross section and the top views of the samples, where  $d$  is the diameter of the pinhole penetrating the  $\text{SiO}_2$  layer. (b) and (c) Scanning electron micrographs of the pinholes penetrating the  $\text{SiO}_2$  layer.

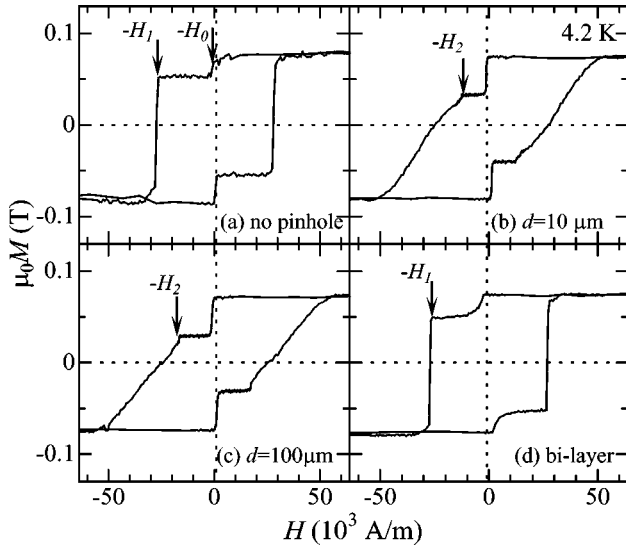


FIG. 2. Magnetization ( $M$ ) curves at 4.2 K for  $\text{SmCo}_5/\text{SiO}_2/\text{Fe}_{19}\text{Ni}_{81}$  trilayer films with (a)  $d=0$ , (b)  $10\ \mu\text{m}$ , and (c)  $100\ \mu\text{m}$ , and (d) a  $\text{SmCo}_5/\text{Fe}_{19}\text{Ni}_{81}$  bilayer film. The external magnetic field ( $H$ ) is applied along the easy axis of the  $\text{SmCo}_5$  layer in the film plane. The arrows indicate irreversible magnetization processes (see text).

Figures 2(a)–2(d) show the magnetization curves at 4.2 K for  $S_0$  (no pinhole),  $S_{10}$ ,  $S_{100}$ , and a  $\text{SmCo}_5/\text{Fe}_{19}\text{Ni}_{81}$  bilayer film which is presumed to have a pinhole with infinite diameter ( $S_\infty$ ). An external magnetic field  $H$  was applied along the easy axis of the  $\text{SmCo}_5$  layer in the film plane. In the absence of the pinhole ( $S_0$ ), when a magnetic field in the negative direction is applied to the system magnetized in the positive direction, a first steep change of magnetization appears at a negative field  $-H_0$  [Fig. 2(a)], which corresponds to the magnetization reversal field in the soft-ferromagnetic  $\text{Fe}_{19}\text{Ni}_{81}$  layer.<sup>7</sup> The magnetization change at a field  $-H_1[S_0]$  higher than  $-H_0$  is due to the uniform rotation of the magnetic moment in the hard-magnetic  $\text{SmCo}_5$  layer.<sup>7</sup> In the system  $S_{10}$  [Fig. 2(b)], on the other hand, the change at  $-H_1$  disappears and the magnetization decreases gradually below  $-H_2[S_{10}] = -13\ \text{kA/m}$ . Since the magnetization curve in the field range  $H < -H_2[S_{10}]$  exhibits irreversible variation (not shown here), the cusp at  $-H_2[S_{10}]$  and the change of magnetization in the range  $H < -H_2[S_{10}]$  are attributable to the domain nucleation in the hard-magnetic  $\text{SmCo}_5$  layer and the propagation of the domain wall, respectively. The magnetization for  $S_{100}$  exhibits a cusp around  $17\ \text{kA/m}$ , which is larger than  $H_2[S_{10}] = 13\ \text{kA/m}$  [see Fig. 2(c)]. This implies that the increase in the interface size suppresses domain nucleation (see below). With further increase of  $d$ , the domain-nucleation behavior disappears, and the magnetization curve turns into the feature characteristic of the uniform magnetization reversal in each layer, typically observed in the bilayer sample without the  $\text{SiO}_2$  layer [see Fig. 2(d)]. Such a  $d$  variation in the magnetization curves indicates that a micron-size pinhole gives rise to domain nucleation and that it significantly changes the whole magnetization process of the  $\text{SmCo}_5$  layer. The disappearance of

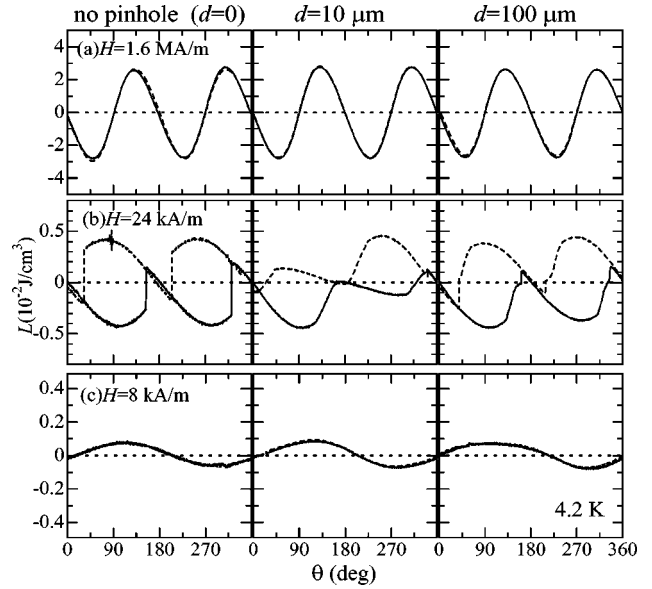


FIG. 3. Magnetic torque ( $L$ ) curves at 4.2 K for  $\text{SmCo}_5/\text{SiO}_2/\text{Fe}_{19}\text{Ni}_{81}$  trilayer films with  $d=0$ ,  $10$ , and  $100\ \mu\text{m}$ . The external magnetic field ( $H$ ) was applied to the film plane. The zero angle  $\theta=0$  is defined as the direction parallel to the easy axis of the  $\text{SmCo}_5$  plane.

the uniform magnetization switching in the  $\text{SmCo}_5$  layer of samples with the pinhole can be accounted for by the static magnetic interaction across the domain wall due to the multidomain structure for  $H < -H_2$  in the  $\text{SmCo}_5$  layer.

The domain nucleation around the pinhole is observed more clearly in the magnetic torque. Figures 3(a)–3(c) exemplify the magnetic torque curves  $L(\theta)$  at 4.2 K for  $S_0$ ,  $S_{10}$ , and  $S_{100}$ . The external magnetic field  $H$  was applied to the plane. The origin of  $\theta$  is defined as the direction along the easy axis of the  $\text{SmCo}_5$  plane. Before the measurement, a magnetic field of  $1.6\ \text{MA/m}$  much higher than  $H_1$  was applied along the  $\theta=0$  direction, where the magnetization in both layers is almost saturated, and the torque curves show a twofold rotational symmetry as  $L(\theta) = -K_u \sin(2\theta)$ , reflecting the uniaxial magnetic anisotropy  $K_u$  in the  $\text{SmCo}_5$  layer. On the other hand, at  $H = 8\ \text{kA/m}$  ( $\ll H_2$ ), where the magnetization in the  $\text{SmCo}_5$  layers is hardly affected by the external magnetic field, each torque curve exhibits a onefold rotational symmetry due to the static magnetic coupling energy ( $E_{\text{sm}}$ ) between  $\text{Fe}_{19}\text{Ni}_{81}$  and  $\text{SmCo}_5$  layers. Important is that both the torque curves at  $H \gg H_1[S_0]$  and  $H \ll H_2$  scarcely vary with  $d$ . This confirms that  $K_u$  as well as  $E_{\text{sm}}$  for the present systems are almost identical. Nevertheless, the torque curves at  $H = 24\ \text{kA/m}$  ( $H_2 < H \ll H_1[S_0]$ ) are heavily dependent on  $d$ , as shown in Fig. 3(b). The torque curves at  $H = 24\ \text{kA/m}$  are characterized by a deviation from the sinusoidal variation and the emergence of rotational hysteresis with respect to  $\theta$ . In this field range, the magnetization of the  $\text{SmCo}_5$  layer deviates from the field direction, which causes the rotational hysteresis. For better comparison, the torque curves as a function of  $d$  are shown in Fig. 4(a). In the absence of the pinhole  $S_0$ , when  $\theta$  is increased, a steep

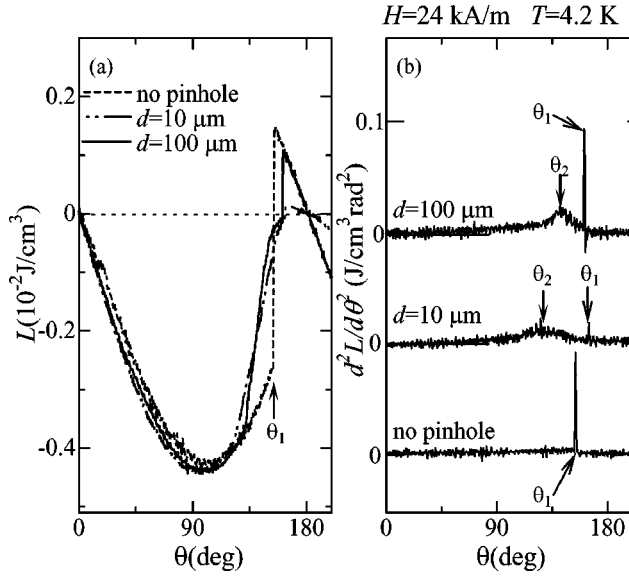


FIG. 4. (a) The pinhole-size dependence of magnetic torque ( $L$ ) curves at 4.2 K for  $\text{SmCo}_5/\text{SiO}_2/\text{Fe}_{19}\text{Ni}_{81}$  trilayer films. The external magnetic field was applied to the film plane. The zero angle  $\theta = 0$  is defined as the direction along the easy axis of the  $\text{SmCo}_5$  layer. The torque  $L$  was measured with increasing  $\theta$ . The arrows indicate the irreversible magnetization processes (see text). (b) The pinhole-size dependence of  $d^2L(\theta)/d\theta^2$  at 4.2 K. The angles  $\theta_1$  and  $\theta_2$  indicate the positions of the sharp and broad peaks, respectively.

change of  $L(\theta)$  appears at  $\theta_1[S_0] = 155^\circ$ , corresponding to the uniform magnetization switching in the  $\text{SmCo}_5$  layer. In the sample with a pinhole, on the other hand,  $L(\theta)$  starts deviating from the sinusoidal variation and increases rapidly far below  $\theta_1[S_0]$  [see Figs. 3(b) and 4(a)]. To show the change more clearly, we have plotted  $d^2L(\theta)/d\theta^2$  deduced from  $L(\theta)$  measured with increasing  $\theta$ , shown in Fig. 4(b). The sharp peak structure of  $d^2L(\theta)/d\theta^2$  observed in  $S_0$  at  $\theta_1[S_0] = 155^\circ$  corresponds to the aforementioned uniform switching of the magnetic moment in the  $\text{SmCo}_5$  layer. The appearance of broad peak structures of  $d^2L(\theta)/d\theta^2$  was noticed at around  $\theta_2 = 125^\circ$  and  $145^\circ$  in  $S_{10}$  and  $S_{100}$ , respectively, indicating anomalously steep increases in the slope of  $L(\theta)$  around  $\theta_2$ . The angle  $\theta_2$  is equal to the angle where  $L(\theta)$  starts deviating from the sinusoidal shape. It should be noted that such a broad peak disappears in the absence of the pinhole. This means that the broad peak of  $d^2L(\theta)/d\theta^2$  around  $\theta_2$  corresponds to the domain nucleation at the pinhole in the  $\text{SmCo}_5$  layer. The rapid increase in  $L(\theta)$  for  $\theta_2 < \theta \leq 170^\circ$  is attributed to the domain expansion. With further increases in  $\theta$ , abrupt jumps of  $L(\theta)$  appear at  $\theta_1 = 170^\circ$  and  $160^\circ$  in  $S_{10}$  and  $S_{100}$ , respectively [see Figs. 4(a) and 4(b)]. The jumps of  $L(\theta)$  are attributed to the uniform magnetization switching in a part of the area outside the expanding domain in  $\text{SmCo}_5$  layer. The discrepancy between

$\theta_1[S_0]$  and  $\theta_1[S_{10}, S_{100}]$  can be accounted for by the magnetic interaction arising from the multidomain structure in the  $\text{SmCo}_5$  layer of  $S_{10}$  and  $S_{100}$ . In  $S_{10}$ , the torque curve for  $180^\circ < \theta < 360^\circ$  is observed to be different from that for  $0^\circ < \theta < 180^\circ$ , indicating a residual multidomain structure around  $\theta = 180^\circ$  in the  $\text{SmCo}_5$  layer of  $S_{10}$ . Such a suppression of the magnetization switching due to the multidomain structure, which also manifests itself in the magnetization curves as the disappearance of the steep change at  $-H_1$ , critically changes the area of the hysteresis in the torque curves as well as the hysteresis loss energy.

Finally, let us briefly discuss the  $d$ -dependent behavior of the domain nucleation arising from the pinhole. As mentioned above, observed  $H_2$  and  $\theta_2$  increase with increasing  $d$ ;  $H_2[S_{10}] = 13 \text{ kA/m} < H_2[S_{100}] = 17 \text{ kA/m}$  or  $\theta_2[S_{10}] = 125^\circ < \theta_2[S_{100}] = 145^\circ$ . This suggests that the increase in the interface size suppresses the domain nucleation. Such  $d$  dependencies of  $H_2$  and  $\theta_2$  are argued from the viewpoint of nucleation of a single domain as follows. Assuming a nucleation of a single domain of identical size to the pinhole, the condition of the nucleation around the pinhole has two requirements: (i) the energy change of the domain nucleation,  $\Delta$ , is negative, and (ii) the threshold energy of the nucleation,  $E_{TH}$ , is smaller than the thermal fluctuation energy per a degree of freedom<sup>8</sup> ( $\approx k_B T/2$ ). Concerning requirement (i), the  $d$  dependence of  $\Delta$  cannot be responsible for the observed variation of  $H_2$  and  $\theta_2$ , since  $\Delta$  is, rather, enhanced by increasing the size of the nucleated domain. Concerning requirement (ii), on the other hand, the nucleation field  $H_2$  or  $\theta_2$  is enhanced by increasing  $d$  when  $k_B T \ll E_{TH}(H=0)$ , since  $E_{TH}$  is enhanced by increasing the size of the nucleated domain. This suggests that the increase in the nucleation size as a result of the increase in the pinhole size gives rise to the observed enhancement of  $H_2$  or  $\theta_2$ . In other words, the  $d$  variation of the magnetization process in the present study may be a reflection of the competition between the pinhole size and the typical dimension that can be thermally nucleated. Such competition can be responsible for the variation in the magnetization process and the change in the coercive force in the hard-magnetic layers.

In summary, the magnetization process for hard-magnetic  $\text{SmCo}_5/\text{SiO}_2/\text{soft-magnetic Fe}_{19}\text{Ni}_{81}$  trilayer films was investigated, wherein the size of the interface between magnetic layers was controlled by the dimension of a pinhole penetrating the  $\text{SiO}_2$  layer. The observed magnetization curves and the magnetic torque curves indicate that even a micron-sized pinhole gives rise to the domain nucleation and significantly changes the whole magnetization process in the  $\text{SmCo}_5$  layer whose diameter is  $\sim 300$  times as large as that of the pinhole. The pinhole-size dependence of the domain-nucleation field is accounted for by the variation in the threshold energy of the nucleation.

This work was supported by a Grant-in-Aid from the Ministry of Education, Science, and Culture of Japan.

- <sup>1</sup>E.F. Kneller, IEEE Trans. Magn. **27**, 3588 (1991).
- <sup>2</sup>J. Nogues and Ivan K. Schuller, J. Magn. Magn. Mater. **192**, 203 (1999).
- <sup>3</sup>M. Amato, M.G. Pini, and A. Rettori, Phys. Rev. B **60**, 3414 (1999).
- <sup>4</sup>K. Mibu, T. Nagahama, T. Shinjo, and T. Ono, J. Magn. Magn. Mater. **177-181**, 1267 (1998).
- <sup>5</sup>E.E. Fullerton, J.S. Jiang, M. Grimsditch, C.H. Sowers, and S.D. Bader, Phys. Rev. B **58**, 12 193 (1998).
- <sup>6</sup>R. Skomski and J.M.D. Coey, Phys. Rev. B **48**, 15 812 (1993).
- <sup>7</sup>A. Wuchner, J. Voiron, J.C. Toussaint, and J.J. Prejean, J. Magn. Magn. Mater. **148**, 264 (1995).
- <sup>8</sup>L. Néel, Rev. Mod. Phys. **25**, 293 (1953).